Photocycles of bacteriorhodopsin in light- and dark-adapted purple membrane studied by time-resolved absorption spectroscopy

James Hofrichter, Eric R. Henry, and Richard H. Lozier
Laboratory of Chemical Physics, National Institute of Diabetes and Digestive and Kidney Diseases, National Institutes of Health, Bethesda, Maryland 20892

ABSTRACT Nanosecond time-resolved absorption spectra have been measured throughout the photocycle of bacteriorhodopsin in both light-adapted and dark-adapted purple membrane (PM). The data from dark-adapted samples are interpretable as the superposition of two photocycles arising independently from the all-*trans* and 13-*cis* retinal isomers that coexist in the dark-adapted state. The presence of a photocycle in dark-adapted PM which is indistinguishable from that observed for light-adapted PM under the same experimental conditions is demonstrated by the observation of the same five relaxation rates associated with essentially identical changes in the photoproduct spectra. This cycle is attributed to the all-*trans* component. The cycle of the 13-*cis* component is revealed by scaling the data measured for the light-adapted sample and subtracting it from the data on the dark-adapted mixture. At times <1 ms, the resulting difference spectra are nearly time-independent. The peak of the difference spectrum is near 600 nm, although there appears to be a slight (~2 nm) blue-shift in the first few microseconds. Subsequently the amplitude of this spectrum decays and the peak of the difference spectrum shifts in two relaxations. Most of the amplitude of the photoproduct difference spectrum (~80%) decays in a single relaxation having a time constant of ~35 ms. The difference spectrum remaining after this relaxation peaks at ~590 nm and is indistinguishable from the classical light-dark difference spectrum, which we find, in experiments performed on a much longer time scale, to peak at 588 nm. The decay of this remaining photoproduct is not resolvable in the nanosecond kinetic experiments, but dark adaptation of a completely light-adapted sample is found to occur exponentially with a relaxation time of ~2,000 s under the conditions of our experiments.

INTRODUCTION

Bacteriorhodopsin (bR), the light-driven photon pump from the purple membrane (PM) of the halophilic bacterium *Halobacterium halobium,* contains a retinal chromophore which is attached to lysine 216 of the opsin protein by a protonated Schiff base linkage (for reviews see Stoeckenius et al., 1979; Birge, 1981; Stoeckenius and Bogomolni, 1982). In the light-adapted state, the retinal chromophore is in the all-*trans* configuration, with an absorption maximum at 568 nm. Absorption of a photon initiates a photocycle which results in the pumping of protons across the cell membrane. Photoactivation converts a fraction of the excited retinal to a photoproduct, commonly referred to as '*K*', in which the retinal has the 13-*cis* conformation (Braiman and Mathies, 1982; Smith et al., 1984; Smith et al., 1986). The *K* intermediate decays along a complex path containing a sequence of intermediates, which are conventionally labeled '*L*', '*M*', and '*N*', in which the retinal conformation has also been identified to be 13-*cis* by time-resolved Raman studies (Braiman and Mathies, 1982; Smith et al., 1984; Smith et al., 1986; Fodor et al., 1988). The retinal reisomerizes to all-*trans* in forming the '*O*' intermediate (Smith et al., 1983) before recycling back to the initial light-adapted bR molecule (Lozier et al., 1975; Nagle et al., 1982; Mauer et al., 1987 *a*, *b*).

The cycle of the light-adapted bR molecule has been extensively studied using a wide variety of techniques (see reviews cited above). The pathway by which light-adapted bR is formed from the equilibrium state to which PM relaxes in the absence of light (i.e., "dark-adapted" bR) is less well characterized. When dark-adapted, the absorption spectrum of the retinal shifts to ~ 560 nm and between 50 and 70% of the 13-*cis* isomer is isolated upon extraction and analysis of the chromophore (Dencher et al., 1976; Maeda et al., 1977; Sperling et al., 1977; Scherrer et al., 1987, 1989). ^{13}C nuclear magnetic resonance (NMR) spectra of the dark-adapted mixture also show the presence of ~60% of the 13-*cis*, 15-*syn* isomer (Harbison et al., 1984). Accurate characterization of the response of bR in dark-adapted PM to photoexcitation has proven to be difficult, in part because of the presence of this mixture of species (Kalisky et al., 1977; Iwasa et al., 1981). An alternative approach has been to study bacterio-opsin reconstituted with the pure 13-*cis* isomer of retinal. This approach is complicated by a different problem: the possibility of sample heterogeneity intro-

0006-3495/89/10/693/14 $2.00

duced by the reconstitution procedure. The reconstituted molecule exhibits an absorption maximum in the range 548–555 nm (Sperling et al., 1977; Scherrer et al., 1989). Photoexcitation studies of the reconstituted 13-*cis* bR at low and room temperatures have revealed a red-shifted photoproduct with a difference peak at ~610 nm which decayed to a mixture of 13-*cis* bR and all-*trans* bR in ~50 ms at 20°C and pH 6.9 (Sperling et al., 1977; Iwasa et al., 1981). Recent Fourier-transform infrared absorption studies have shown that the retinal conformation in this photoproduct is predominately all-*trans,* 15-*syn* (Roepe et al., 1988).

It is important to characterize the photocycle of dark-adapted PM for several reasons. The first is that formation of light-adapted bR from dark-adapted bR is the first step in the photocycle of functioning PM. One would like to understand quantitatively all of the kinetic processes that are involved in the transformation of PM from the dark-adapted, equilibrium state to the light-adapted, metastable state. A second point is the general assumption that light-adapted PM is homogeneous and contains only a single molecular species. The existing data on the kinetics of light- and dark- adaptation are controversial on this point, with the interconversion between the two states reported to be kinetically complex in some studies (Kalisky et al., 1977; Casadio et al., 1980), and to follow simple relaxation kinetics in others (Oesterhelt et al., 1973; Scherrer et al., 1989). A third is that studies of the dark-adapted mixture can address the question of the dependence of the photocycle of bR on the structural state of neighboring bR molecules. If the cycle is completely decoupled from the conformational state of other bR molecules in the membrane, then it follows that the photocycle of the all-*trans* component of dark-adapted PM should be identical to that observed for light-adapted PM. A careful study of the photocycle of the dark-adapted mixture thus provides a sensitive probe for the existence of functional interactions between neighboring bR molecules. Finally, the characterization of the photocycle of light-adapted PM is being carried out to such high experimental precision (e.g., Xie et al., 1987; Mauer et al., 1987*a*) that it is important to know to what extent a very small fraction of the 13-*cis* isomer, present as a result of incomplete light-adaptation, would affect the results of these experiments. To answer this question, one needs to know both the difference spectra and relaxation kinetics of the photoproducts of the 13-*cis* component of dark-adapted PM.

Here we report time-resolved absorption spectra of dark-adapted purple membrane measured with 10 ns resolution. The kinetics of the early portions of the photocycle of dark-adapted PM (10 ns – 1 ms) can be qualitatively explained by adding a single photoproduct-reactant difference spectrum to the difference spectra measured for the photocycle of light-adapted bR. This early difference spectrum is red-shifted from the light-dark difference spectrum which is normally measured on the time scale of minutes (Oesterhelt et al., 1973; Bogomolni et al., 1980) and decays by depletion of its red edge, with the principal relaxation occurring at ~35 ms. Based on the close correspondence between the observed cycle and that of 13-*cis* bR originally characterized by Sperling et al. (1977) using bacterio-opsin reconstituted with 13-*cis* retinal, we assign this spectrum to a photoproduct of the 13-*cis* component of the dark-adapted PM. No clearly distinguishable spectral features are observed at other wavelengths during the decay of this photoproduct, suggesting that the spectra of the intermediates in the 13-*cis* photocycle are similar to that of all-*trans* retinal in light-adapted PM, but are slightly red-shifted and exhibit somewhat higher peak extinction coefficients.

EXPERIMENTAL

Time-resolved spectra were measured with a spectrometer that has been previously used for flash-photolysis studies of heme proteins (Hofrichter et al., 1983; 1985; Murray et al., 1988). Here we briefly describe the instrument, some recent improvements, and the modifications required for the studies of bacteriorhodopsin. The instrument utilizes two Q-switched Neodymium:YAG lasers. The 355 nm third harmonic of the first (pump) laser (Quanta Ray DCR 1A; Spectra Physics, Mountain View, CA) was used to excite the bR sample. The second (probe) laser, which was delayed electronically with respect to the pump laser, was used to generate a short (10 ns) white light flash which is used to measure the absorption spectrum of the sample. To do so, the third harmonic output of the probe laser (Quanta Ray DCR 1) was used to excite a mixture of fluorescent dyes which contained stilbene 420, brilliant sulfaflavine, rhodamine 560, rhodamine 610, and cresyl violet dissolved in methanol, which was slowly circulated thorugh a capillary tube with an inside diameter of 0.010 inch. This dye mixture produced a 300 nm wide emission spectrum (390–690 nm) with an intensity, after collection and dispersion to a resolution of 2 nm, of $\sim 10^7$ photons/pulse/nm. Excitation at 355 nm was chosen to permit acquisition of absorption spectra over the entire bandwidth of this light source.

The output light from the dye cell was focused onto a slit-shaped volume of the sample that contained both a excited and unexcited region and was subsequently focussed onto the 50 μm entrance slit of a 0.25 meter spectrograph (Jobin-Yvon M-25; Instruments SA, Metuchen, NJ) with a low dispersion, 162 g/mm holographic grating. The dispersed output from the spectrograph was collected on a silicon vidicon tube with extended red sensitivity (PAR 1252E; EG&G Princeton Applied Research, Princeton, NJ) and read by an OMA detector controller (PAR 1216). The controller was interfaced to an HP 9826 calculator (Hewlett-Packard Co., Fort Collins, CO) which was programmed to collect, average and store the measured intensities using Multiforth (Creative Solutions Inc., Rockville, MD), a multi-tasking operating system. Two tracks of intensities were measured, one from the excited and one from an unexcited region of the sample. The logarithm of the ratio of the two intensities at each wavelength thus produces a difference spectrum between the photoproduct and the unexcited sample.

Spectra were measured on a logarithmic grid of times with 12 points/decade. The shortest times preceded temporal coincidence of the two laser pulses and the longest times were determined by the time

required for completion of the photocycle (or a maximum of 500 ms). To reach these delays, the repetition rate of the Q-switched output of both lasers was reduced below the 10 Hz repetition rate at which the laser flashlamps were fired by a counter that triggered the Q-switch only after a cycle consisting of n pulses of the flashlamps, where n could be varied from 1 to 16. Intensities from a total of 20 probe laser shots were averaged to produce each spectrum. The average of four shots was accumulated on the vidicon before reading each exposure and the results of five exposures were summed in the HP 9826. The intensity data were spooled via Ethernet to a model 3 computer (Sun Microsystems, Mountain View, CA) for processing and analysis. The first step in the analysis was to calculate difference absorption spectra from the intensity data. To do so, the dark counts were subtracted from the measured intensities and the log ratio of the intensities from the two tracks was calculated. The appropriate baselines measured on the unphotolyzed sample were then subtracted. The noise in the determination of the ΔOD at a given wavelength and time is $\sim \pm 10^{-3}$ O.D.

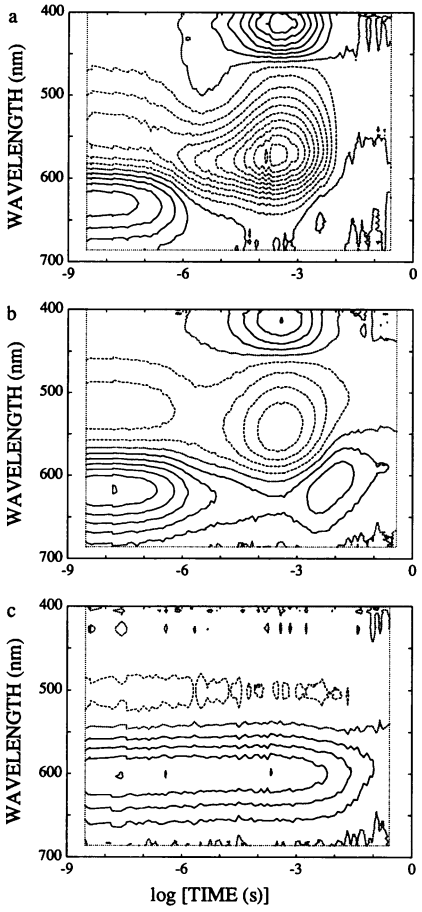

FIGURE 1 Averaged data measured on light-adapted (a) and dark-adapted (b) PM at pH 7.3 and 25 C and the difference obtained after scaling and subtraction (c). Each of the measured spectral surfaces (a, b) was obtained by averaging four identical data sets. Each data set consisted of Δo.d. measurements at 400 wavelengths and ~100 time points. The data in the contour plots have been averaged over the ~1.5 nm spectral resolution of the spectrograph (two wavelength points). Contours are shown at 0.01 o.d. intervals with negative contours shown as dashed, zero contours shown as dotted and positive contours as solid lines. The details of the procedure used to calculate the difference data (c) are presented in Results.

The resulting set of time-resolved absorption difference spectra were analyzed by singular value decomposition (SVD) and nonlinear least-squares fitting of the resulting time-dependent amplitudes to sums of exponential relaxations using a procedure similar to that previously described (Hofrichter et al., 1985). SVD is a matrix rank-reduction algorithm that is used to condense the time-dependent information from kinetics measured at 400 wavelengths into a small number of time-dependent amplitude vectors (V's) (Press et al., 1986). These vectors are then fitted using a simultaneous nonlinear least squares fitting program. The fitting algorithm included a procedure similar to that described by Mauer et al. (1987a), in which, given a set of successful fits to the kinetic data using n exponential relaxations, the fits are first sorted, using the final weighted sum of squared residuals as a measure of the goodness-of-fit. An additional relaxation is then introduced into the best n-relaxation fit, using $n + 1$ different initial values for its relaxation rate, one chosen in each possible rank-ordered position relative to the rates from the previous fit. In the fitting procedure, the squared residuals from each set of time-dependent amplitudes (columns of V) were weighted by the squares of the singular values. We compared the SVD compression technique with the published analysis of the data of Xie et al. (1987) and found that fully consistent results are obtained by the two procedures.

The PM sample was a gift from D. Oesterhelt. The sample was suspended at a concentration of ~0.3 mM bR in a buffer consisting of 1 mM sodium acetate, 1 mM sodium phosphate, 1 mM sodium borate, and 7 mM sodium chloride adjusted to pH 7.3. In order to minimize shot-to-shot variations in photolysis amplitude the sample was excited with an absorbed pulse energy of ~8 mj, which results in ~10 photons absorbed/molecule/pulse. This absorbed energy is sufficient to pump light-adapted PM to a photostationary state. We found in preliminary experiments that extensive exposure of light-adapted PM suspensions to these pulses bleached the 568 nm peak of the sample, producing a permanently red-shifted photoproduct. The apparent rate of formation of this product at 25 C was found to be very low (<0.0002/pulse) but too high to permit a complete data set to be accumulated on a single sample. For this reason, the suspension was circulated through an aqueous electron paramagnetic resonance cell having a pathlength of 0.35 mm (Wilmad) by a peristaltic pump which was synchronized with the firing of the lasers. A fresh 20 μl sample of the suspension was pumped into the observed position of the cuvette during the interval between reading the vidicon and firing the lasers for the next set of four exposures. In this way an individual membrane fragment was only exposed to a small number of photolysis pulses before being recycled to the sample reservoir (total volume ~5 ml) and measurable accumulation of this low-yield photoproduct was prevented. Orientation of the membrane lamellae by the flow-induced shear field could be observed from the increase in sample absorbance. The relaxation time for the orientation was several seconds. This slow rotational relaxation coupled with relatively high excitation energy minimizes the sensitivity of the experiment to chromophore motions. The sample temperature was controlled by a copper sandwich placed over the cell, which was, in turn, controlled by a circulating bath. When desired, light-adaptation of the sample entering the cell was accomplished by illuminating the tubing connecting the darkened sample reservoir with the cell with a fluorescent desk lamp and illuminating the entrance capillary of the cell with a 2 mw helium-neon laser.

RESULTS

Time-resolved absorption difference spectra collected through the cycles of light- and dark-adapted bR are

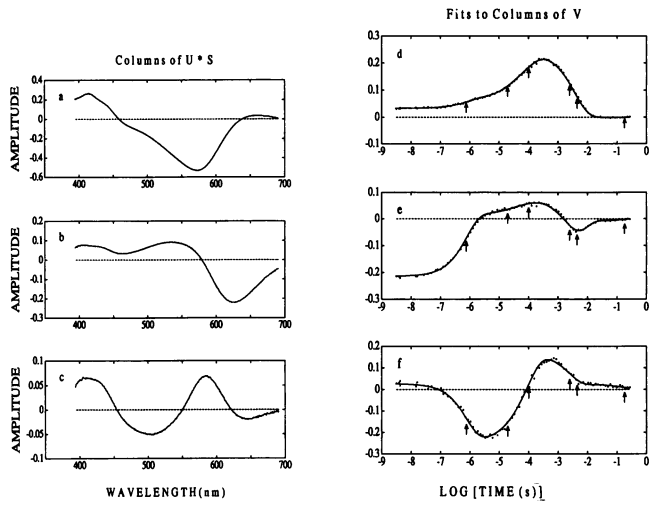

FIGURE 2 Singular value decomposition of the time-resolved difference between the spectra of the photoproducts of light-adapted PM and the starting material (Fig. 1 *a*). Data were measured at 100 time points on a logarithmic grid ranging from a time ~10 ns before coincidence of the pump and probe laser pulses to 290 ms after photoexcitation. (*a–c*) The columns of the U*S matrix. These columns are the rank-ordered basis spectra that provide the best least-squares fit to the experimental data shown in Fig. 1 *a*. The singular values associated with the five largest basis spectra were 5.29, 2.12, 0.79, 0.133, and 0.055. (*d–f*) The columns of V. The data points are the amplitudes of the basis spectra which produce the best fit to the spectra measured at each time point. The solid lines show the simultaneous fit of these three columns of V to a sum of six exponential relaxations. The relaxation times are indicated by the arrows and relaxation rates are given in Table 1. Only the data at times greater than the point at which maximum photolysis occurred have been fit and plotted. The delay time of the first retained spectrum was set to 3 ns: the experimental point selected as the time at which photoexcitation was complete was determined from the rise in the amplitude of V column 2 (panel *e*). The measured difference spectra can be calculated as $(\Delta\text{o.d.}(\lambda, t) = \Sigma\ U^*S_j(\lambda)^*V_j(t)$. The maximum Δo.d. measured in this experiment was ~0.1 o.d. a few hundred microseconds after photoexcitation, as seen in Fig. 1 *a*.

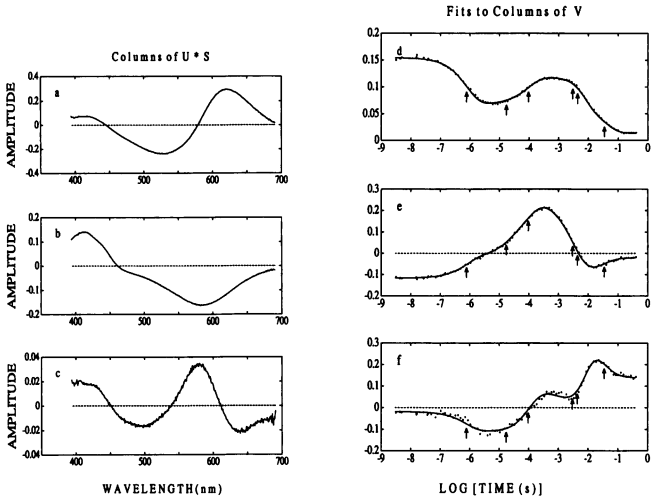

FIGURE 3 Singular value decomposition of the time-resolved difference between the spectra of the photocycle intermediates of dark-adapted PM and the starting material (Fig. 1 *b*). A total of 102 spectra were collected to a maximum delay of 390 ms after photoexcitation. (*a–c*) The columns of the U*S matrix. The singular values associated with the five largest basis spectra were 3.32, 2.00, 0.335, 0.11 and 0.079. (*d–f*) The columns of V. The points are the amplitudes of the basis spectra which produce a best fit to the measured spectrum at each time point. The solid lines show the simultaneous fit of these three columns of V to a sum of seven exponential relaxations. The relaxation rates are given in Table 1. The delay time for the first retained spectrum was chosen as described in Fig. 2 except that the point of completion of photoexcitation was chosen from V column 1 (panel *d*). The maximum Δo.d. measured in this experiment was ~0.06 o.d. for the immediate photoproduct.

shown in Fig. 1.[1] The spectra of light-adapted bR (Fig. 1 *a*) show the expected features resulting from the classic $K \rightarrow L \rightarrow M \rightarrow O \rightarrow$ bR photocycle (Lozier et al., 1975; Mauer et al., 1987*a*, *b*). The spectra of the dark-adapted sample (Fig. 1 *b*) show, in addition, a large, long-lived, red-shifted intermediate which is reminiscent of the ^{610}C photoproduct of 13-*cis* bR originally reported by Sperling et al. (1977). The results of SVD analysis of these data are shown in Figs. 2 and 3. In each experiment we find three significant SVD components. That is, three linearly independent basis spectra are needed to reproduce all of the observed spectra to within the accuracy of the measurement, which is ~±2%. This result requires that a minimum of three distinct spectral species, in addition to light-adapted PM which is the reference sample used for measuring the difference spectra, be present at some point in both the light and dark cycles. This result cannot rule out the possibility that the cycle contains a larger number of kinetic intermediates (Lozier et al., 1975; Nagle et al., 1982; Mauer et al., 1987*a*; Xie et al., 1987). If a larger number of intermediates do exist, then it must be possible to describe the difference spectra of all of the intermediates as linear combinations of the spectra of some subset of three to within the accuracy of the experiments.

The results of analyzing these data by fitting the time-dependent amplitudes of the basis spectra (columns of V) to sums of exponential relaxations are shown in Figs. 2 and 3. The resulting relaxation rates are given in Table 1. Under most conditions, the data on light-adapted samples (Fig. 2, *d* and *f*) could be well-reproduced by using five relaxation times, together with the associated changes in the photoproduct absorption spectra, to fit the experimental data. The averaged data presented here

[1]In preparing the averaged datasets, the data from each experiment being considered for inclusion in the average was first screened by SVD analysis, fitting and calculation of the spectral changes associated with each relaxation to ensure that the information obtained from each data set was identical to within experimental error.

TABLE 1 Relaxation rates obtained from fits (s^{-1})

Light-adapted purple membrane

Fit to five relaxations:

k_I	k_{II}	k_{III}	k_{IV}	k_V
1.28 ± .04 (10^6)	5.2 ± 1.0 (10^4)	9.9 ± 0.7 (10^3)	334 ± 25	213 ± 16

Final weighted sum of squared residuals: 0.0279

Fit to six relaxations:

k_I	k_{II}	k_{III}	k_{IV}	k_V	k_{VI}
1.27 ± .04 (10^6)	4.89 ± 1.0 (10^4)	9.5 ± 0.7 (10^3)	333 ± 25	215 ± 15	5.2 ± 1

Final weighted sum of squared residuals: 0.0223

Dark-adapted purple membrane

Fit to seven relaxations:

k_I	k_{II}	k_{III}	k_{IV}	k_V	k_{VI}	k_{VII}
1.25 ± .03 (10^6)	5.8 ± .7 (10^4)	1.0 ± .04 (10^4)	327 ± 39	225 ± 22	28 ± 3	0*

Final weighted sum of squared residuals: 0.0101

Dark-adapted - light-adapted

Fit to four relaxations:

k_I	k_{II}	k_{III}	k_{IV}
2.6 ± 0.6 (10^5)	165 ± 41	29 ± 3	0*

Final weighted sum of squared residuals: 0.0119

*The fitted relaxation rate for the slowest relaxation was equal to zero to within the error of its determination.

show, in addition, an offset in V column 2 and V column 3 which is fitted by an additional relaxation having a relaxation rate of ~5 s^{-1}. This relaxation has been included in plotting the results shown in Figs. 2 and 4 *a*. The use of a fifth relaxation to fit the data is justified both by the decrease in the weighted sum of squared residentials from 0.0409 to 0.0279 and by inspection of the residuals from the four-component fit, which show clustered, nonrandom residuals in the fit to V column 2 between relaxations I and II, and in the fit to V column 3 between relaxations II and III. The sixth relaxation is required to fit the offset in V column 2 and V column 3 and its inclusion further reduces the weighted sum of squared residuals to 0.0223. We have interpreted this slow relaxation as resulting from incomplete light adaptation of the sample under our conditions of observation (see below).

The difference spectra between the intermediates which are kinetically resolved by the fit and light-adapted PM are shown in Fig. 4 *a*. For an irreversible, sequential model, kinetic intermediates which have a lifetime that is much longer (i.e., by a factor of at least 20) than the time in which they are formed (i.e., species I, II, and IV) must consist primarily of a single species. The measured difference spectra for these species can then be interpreted as the difference spectra between the metastable photoproducts which exist before the relaxations and the unphotolyzed sample. Using the standard convention for the photocycle intermediates, the first three of these spectra would then be labeled as the spectra of the *K*, *L*, and *M* intermediates. The remaining spectra (associated with photoproduct before relaxations III and V) cannot be readily interpreted in the absence of a kinetic model, since the relaxation rates for the appearance and disappearance of these species differ by less than a factor of 5. Even the simplest kinetic models require that these spectra represent mixtures of the spectra of kinetic intermediates with amplitudes which depend on the rates of the model (cf. Nagle et al., 1982). The spectrum prior to relaxation V, which has previously been interpreted as a mixture of intermediates, including *M*, *N*, and *O*, is particularly uncertain as a result of the near degeneracy of the fourth and fifth relaxation rates at temperatures above 20 C at this pH (see Table 1). The near-degeneracy causes the fitted spectral amplitudes associated with these two relaxations to be highly interdependent. As a result, these spectra are poorly determined and somewhat variable from experiment to experiment.

The results of fitting the data on dark-adapted PM are presented in Fig. 3, *d* and *f*, Fig. 4 *b* and Table 1. Fits to the three columns of V required a total of six exponential relaxations, plus an additional relaxation with a rate that was too slow to be resolved in this experiment. This slow relaxation was characterized in independent experiments

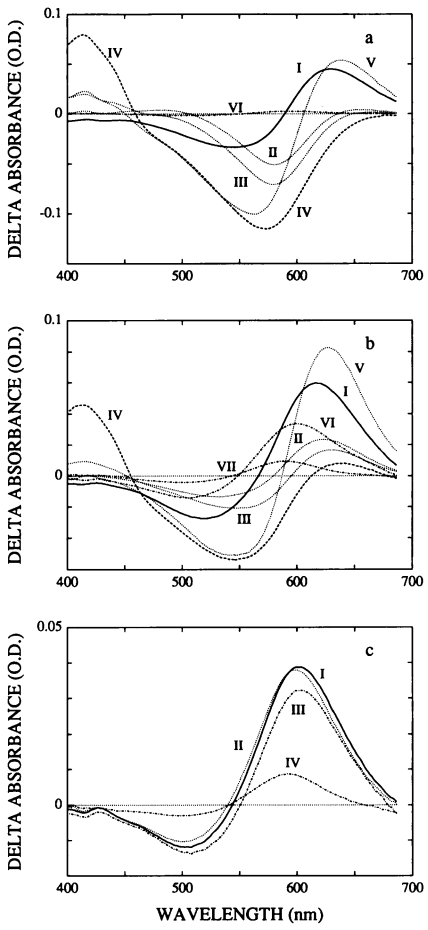

FIGURE 4 Difference spectra obtained from fits to the data in Fig. 1. (*a*) The difference spectra between the intermediates of light-adapted PM and the starting material. (———) The difference spectrum of the immediate photoproduct (before relaxation I). (·····) The difference spectra of the intermediates before relaxations II and III. (-----) The difference spectrum of the intermediate before relaxation IV. (·····) The difference spectrum of the intermediate before relaxation V. (-·-·-) The difference spectrum measured at the conclusion of the experiment. (*b*) The difference spectra between the intermediates of dark-adapted PM and the starting material. The linetypes used for the first five relaxations are identical to those used in (*a*). (-----) The difference spectra of the intermediates prior to relaxation VI and at the conclusion of the experiment. The latter spectrum is the light-dark difference spectrum accumulated during the four exposures of the sample to the pump laser pulse. (*c*) Difference spectra of the photoproducts of the 13-*cis* component of dark-adapted PM. The spectra were obtained from the SVD analysis of the spectral data collected on dark-adapted PM after subtraction of the scaled data for light-adapted PM (Fig. 6): (———) The spectrum before relaxation I; (·····) The spectrum before relaxation II; (-·-·-) The spectrum before relaxation III and the constant spectrum measured after all observable relaxations are complete.

in which the spectrum was monitored after extensive light-adaptation (see below). The use of seven relaxations to fit the data is justified both by the decrease in the final weighted sum of squared residuals from 0.0137 to 0.0101 with the addition of the seventh relaxation, and by inspection of the residuals from the six-component fit, which show clustered, nonrandom residuals in the fit to V column 2 between relaxations I and II, and in the fit to V column 3 in the region of relaxation III. The relaxation rates obtained by fitting the dark-adapted data to a sum of seven exponential relaxations are given in Table 1.

The difference spectra obtained from the fits are shown in Fig. 4 *b*. Recall that, for the dark-adapted PM sample, these spectra describe the time-dependent difference spectra between a mixture of photoproducts and the unphotolyzed dark-adapted PM mixture which contains ~60% 13-*cis* retinal with the remainder in the all-*trans* conformation (Scherrer et al., 1989). The difference spectrum obtained for the immediate photoproduct (I) in Fig. 4 *b* is reminiscent of the K – bR spectrum (I) in Fig. 4 *a*. The same is true of the difference spectrum before the fourth relaxation (IV) in the dark-adapted experiment and the M – bR difference spectrum (IV) in the light-adapted sample. In both cases, however, the difference spectra for the dark-adapted sample are smaller and show a more pronounced red peak. In addition, the unresolved slow relaxation produces a significant offset spectrum at times after the 25 ms relaxation, which is shown as the difference spectrum for relaxation VII in Fig. 4 *b*.

An important clue to the relation between these two sets of data is obtained by comparing the relaxation rates in Table 1. The first five relaxation rates from the fit to the data on dark-adapted PM are, to within the combined errors in their determination, identical to those obtained from the fit to the data on light-adapted PM. This result could be readily explained if the spectra of any photoproducts of the 13-*cis* component of dark-adapted PM were kinetically stable over the time interval during which these five relaxations in the light cycle occur. This hypothesis would also be consistent with the results of Sperling et al. (1977), who found a stable spectrum until ~30 ms after photoexcitation of reconstituted 13-*cis* retinal with bacterio-opsin. The photocycle of dark-adapted PM would then simply be the superposition of the light cycle produced by the all-*trans* retinal isomers and a simpler cycle for the 13-*cis* component which is kinetically silent during most of the light-cycle.

If this hypothesis is correct, then the spectral changes which take place in the two samples during the first five relaxations should also be identical. A comparison of the difference spectra observed for relaxations I – V in the light and dark cycles confirms this expectation. The most accurate comparisons can be made of the spectral

changes occurring in relaxations I and III. The difference spectrum observed for relaxation III for dark-adapted PM is essentially identical to the corresponding spectrum for the 'light' cycle (Fig. 5). The difference spectrum observed during relaxation I is also very similar to the $L - K$ spectrum seen in the light cycle. The only detectable difference is a ~2 nm red shift of the dark $L - K$ difference spectrum. By averaging these spectra and fitting each of the observed difference spectra to the average spectrum, a scale factor of 0.605 was required to match the amplitude of the difference spectra observed in relaxation III for the light cycle to that observed in the dark cycle. The corresponding value for the difference spectra in relaxation I was 0.622.

To further test this hypothesis, the data for the light cycle were scaled to the dark data using the relative amplitudes of the difference spectrum for relaxation III and then subtracted from the dark data. The difference between the data sets is shown in Fig. 1 *c*. As expected, the difference data show an almost constant difference spectrum at times <10 ms which decays at times significantly greater than those required for completion of the light cycle. This data was then analyzed by SVD and simultaneous least squares fitting to the first three columns of V. The results of this analysis are shown in Fig. 6. Nearly 95% of the data can be represented as a single difference spectrum, the shape of which is given by U column 1 (Fig. 6 *a*) The two remaining components are comparable with the noise in the data and the spectral information contained in them is not totally unambiguous (see Discussion). Fits to the dark-minus-scaled-light data required four relaxations. The relaxation rates obtained from the fit are given in Table 1 and the difference spectra before each of the four relaxations are shown in Fig. 4 *c*. These difference spectra are all similar, with minima in the vicinity of 500–505 nm and larger maxima near 600 nm. The difference spectrum of the immediate photoproduct appears to blue shift slightly in relaxation I at ~2 μs, while relaxation II at ~6 ms produces a small, compensating red shift and a small decrease in the amplitude of the difference spectrum. All of the early photoproduct spectra are significantly red-shifted relative to the spectrum before relaxation IV, which closely resembles the light-dark difference spectrum measured at long times (>100 s) (see below). Very similar results were obtained by a different procedure in which the spectra obtained from the independent fits to the light and dark data shown in Fig. 4, *a* and *b* were scaled and subtracted. The primary advantage of the SVD analysis of the difference data is that the time-evolution of the difference spectra arising from the 13-*cis* component of dark-adapted PM can be examined in greater detail and relaxation rates obtained for this evolution.

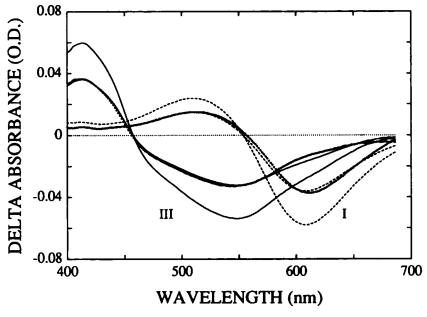

FIGURE 5 Comparison of the early spectral evolution of the intermediates of light-adapted and dark-adapted PM. The difference spectra which result from relaxations I and III for dark-adapted PM (·····) and for relaxations I (-----) and III (———) for light-adapted PM before and after normalization of the light-adapted spectra are shown.

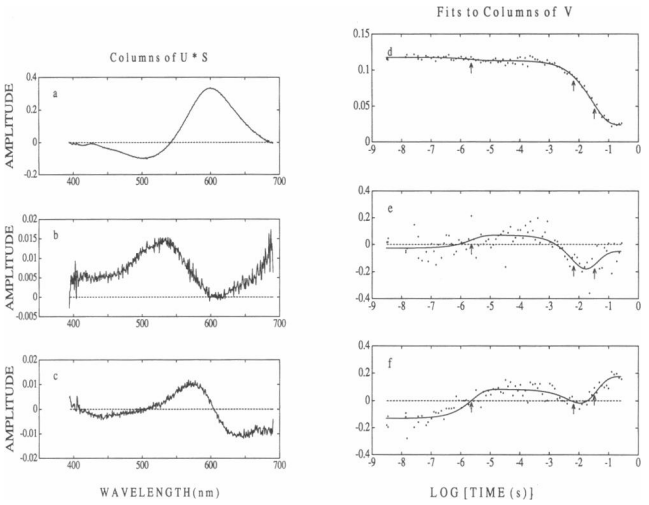

FIGURE 6 SVD analysis of the difference between the dark and scaled light data. The SVD analysis of the data in Fig. 1 *c* generates basis spectra having singular values of 2.96, 0.159, 0.123, and 0.080. The second two components have amplitudes only about a factor of two larger than those discarded in the analysis of the light and dark data sets (Figs. 2 and 3). (*a–c*) The columns of the U*S matrix. (*d–f*) The columns of V. The solid lines show the simultaneous fit of these three columns of V to a sum of four exponential relaxations. The relaxation rates are given in Table 1. The maximum Δo.d. measured in the calculated difference spectra was ~0.04 o.d. for the immediate photoproduct.

Experiments were also carried out to obtain accurate difference spectra for the transformation between the light-adapted and the dark-adapted state. These experiments were carried out in two ways. First, we monitored the spectrum of an unflowed sample as a function of the number of exposures to the pump laser pulse. Second, we monitored the time-evolution of the spectrum of a sample after full light-adaptation. In addition to the light-dark difference spectrum, the first experiment yields the probability that the 13-*cis* component of dark-adapted PM is

converted to a long-lived all-*trans* state by a single pulse of our pump laser (Fig. 7 *a*) and the second experiment yields the relaxation rate for the light ⇄ dark thermal reaction under our experimental conditions (Fig. 7 *b*). A fit of the data in Fig. 7 *a* to a single exponential yields the probability of 0.020/pulse for conversion of 13-*cis* to light-adapted all-*trans* by exposure to our pump pulse. The fit is remarkably good over this range of exposure.

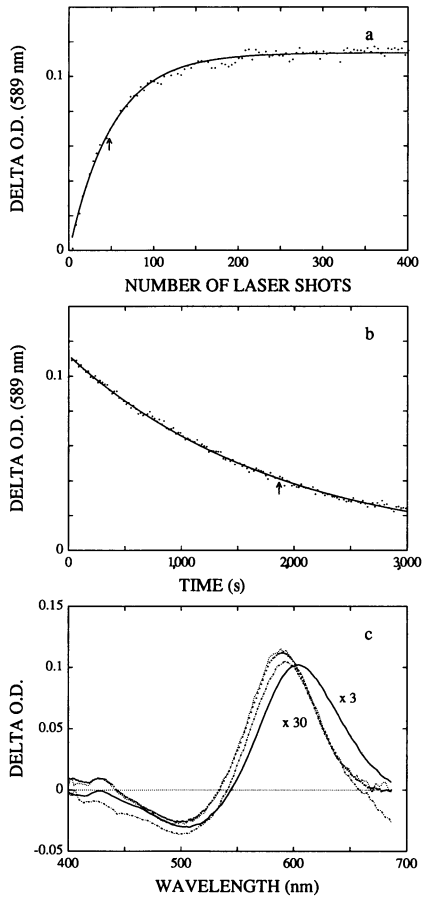

FIGURE 7 The kinetics and spectral changes for light- and dark-adaptation, pH 7.3, 25 C. (*a*) Light-adaptation kinetics measured by successive absorption measurements made 400 ms after photoexcitation. Independent spectra were measured after every four laser shots. SVD analysis of these data produced only a single basis spectrum representing >95% of the measured data. (*b*) Kinetics of dark-adaptation. The decay of the light-dark difference spectrum generated by photoexcitation with 200 shots of the pump laser was monitored by measuring 150 spectra using the probe source only. The interval between experiments was 21 s. The fitted relaxation rate was $5.3(10^{-4}) \pm 1.4(10^{-5})$ s^{-1}. (*c*) Difference spectra obtained from the kinetic experiments. The heavy dotted curve is the difference spectrum obtained in the light-adaptation experiment shown in Fig. 7 *a*. The light dotted curve is the difference spectrum measured in the dark-adaptation experiment (Fig. 7 *b*). (———) The photoproduct—13-*cis* spectrum obtained by correcting the data in Fig. 4 *c*. (-·-·-) The corrected spectrum of the residual photoproduct of the 13-*cis* component subsequent to relaxation III.

Full light adaptation required ~ 250 exposures. To monitor dark-adaptation a sample was first prepared by exposing it to 200 shots of the pump laser at 2.5 Hz and then repetively measuring the difference spectrum at 21-s intervals. The decay in Fig. 7 *b* is well fitted by a single exponential having a relaxation time of 2,000 ± 100 s. This rate for dark-adaptation lies between those reported by Casadio et al. (1980) and by Scherrer et al. (1989). The rate measured in our experiments may be increased slightly by diffusion of the light-adapted PM out of the excited volume. Light-adaptation of the reference portion of the sample by exposure to the probe beam will increase the apparent rate of dark-adaptation by <10%. The difference spectra obtained in these experiments are shown in Fig. 7 *c*. Based on an extinction coefficient of 63 $mM^{-1}cm^{-1}$ for light-adapted bR, the peak change in extinction coefficient in this reaction is 12 mM^{-1} cm^{-1}. The absolute spectra of dark-adapted PM can be calculated from the measured spectra of light-adapted PM and the dark-light difference spectra in Fig. 7 *c*. The absolute spectra for light-adapted and dark-adapted PM are shown in Fig. 8 *a*.

The results in Fig. 7 *a* show that each laser pulse converts ~2.0% of the 13-*cis* bR component of dark-adapted PM to light-adapted bR, containing all-*trans* retinal. This product then decays in ~ 2,000 s, so it is stable throughout the 10 s duration of the data acquisition cycle of our experiments. As a result, the small amount of this product which is generated by the first shot in the cycle persists and is cycled during subsequent flashes of the probe source.[2] This effect has not been taken into account in the calculation of the difference spectra in Fig. 4 *c* which presents the experimental data but has been corrected in the calculation of the spectra of intermediates presented in Figs. 7 *c* and 8 *c*.

[2]To discuss the spectral changes in the 13-*cis* cycle quantitatively, the experimental procedure used to collect the data must be taken into account. Each aliquot of the sample is exposed to a total of four laser shots, and a long-lived photoproduct is produced by each shot. This product accumulates through the sequence of exposures and the absorbance change which results from the presence of the residual photoproduct is added to that which results from the photoproduct formed in the preceeding photoexcitation pulse in all shots except the first. To calculate true photoproduct spectra for the dark-adapted mixture and its 13-*cis* component this residual spectrum must be removed. Since <10% of the 13-*cis* component becomes light-adapted during a measurement cycle, the correction can be made by subtracting the difference spectrum resulting from the accumulated, light-adapted bR from all of the measured difference spectra of the dark-adapted mixture. The fraction of the residual difference spectrum which is not introduced by the previous exposure is equal to $(1 + 2 + 3)/(1 + 2 + 3 + 4)$ or 60% for a four-exposure sequence. This correction reduces the amplitude of spectrum IV of Fig. 4 *c* by 60% and redshifts spectra I-III by ~3–4 nm. The difference spectra in Fig. 4, *b* and *c*, which are the measured data, contain the contribution of this residual difference spectrum. The spectra in Figs. 7 *c* and 8 *c* have been corrected for this effect.

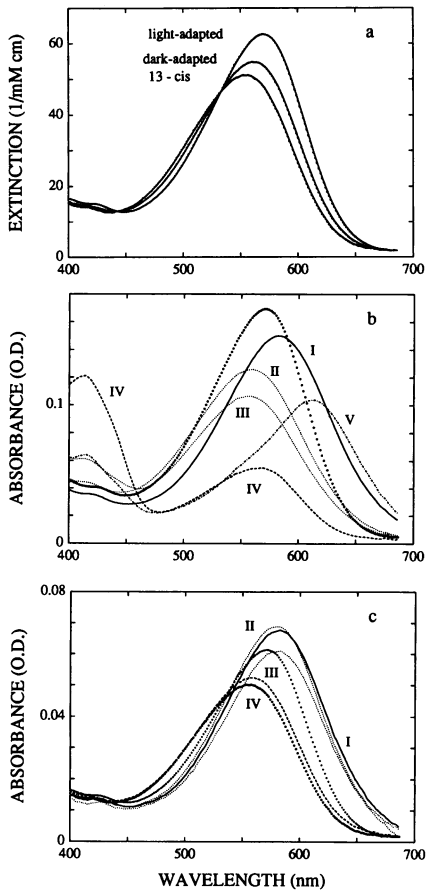

FIGURE 8 Spectra of the all-*trans* and 13-*cis* components of bacteriorhodopsin and the intermediates of their photocycles. (*a*) Spectra of light-adapted and dark-adapted purple membrane and the 13-*cis* component of dark-adapted PM. (·····) The measured spectrum of light adapted PM. (-----) The spectrum of dark-adapted PM calculated from the light-adapted spectrum and the difference spectrum in Fig. 7 *c*. (-·-·-) The spectrum of the 13-*cis* component of dark-adapted PM calculated assuming 60% of the retinal is present as the 13-*cis* isomer. (*b*) The absorption spectra of intermediates in the photocycle of the light-adapted (all-*trans*) isomer. (———) The spectrum of the immediate (*K*) photoproduct (before relaxation I). (·····) The spectra of the intermediates before relaxations II and III. These species have previously been labeled *L* and *L'* (Lozier et al., 1975; Mauer et al., 1987). (-----) The spectrum of the intermediate before relaxation IV. This species is commonly called *M* (Lozier et al., 1975). (-·-·-) The spectrum of the kinetic intermediate prior to relaxation V. This spectrum consists of a mixture of *M*, *N*, and *O* photoproducts (Lozier et al., 1975; Chernavskii et al., 1989). The heavy dotted curve is the scaled spectrum of light-adapted PM (Fig. 8 *a*) which was added to the difference spectra in Fig. 4 *a* to produce the spectra of intermediates shown here. (*c*) The absorption spectra of the intermediates in the 13-*cis* cycle. (———) The spectrum of the immediate photoproduct (before relaxation I). (·····) The spectra of the photoproducts before relaxations II and III. (-----) The residual difference spectrum subsequent to relaxation III. The heavy dotted curve is the scaled spectrum of 13-*cis* component of dark-adapted PM (Fig. 8 *a*) which was added to the corrected difference spectra obtained from the data in Fig. 4 *c* to produce the spectra of intermediates shown here.[2] The medium weight dotted curve is a scaled spectrum of light-adapted bR.

DISCUSSION

The time-resolved spectra shown in Fig. 1 provide a data base that can be used to test assumptions regarding the photocycles of light- and dark-adapted PM. We shall begin by discussing the data on light-adapted PM, proceed to consider the difference data obtained by subtraction of the scaled light data from the dark data and conclude by discussing a number of remaining questions which are raised by the data presented here and previous studies of dark-adapted bR.

The results obtained for light-adapted samples can be fitted using five exponential relaxations. The four relaxation fits correspond closely to early data which was interpreted in terms of a sequential, irreversible

$$K \rightarrow L \rightarrow M \rightarrow O \rightarrow \text{bR}$$

photocycle (Lozier et al., 1975). This model assumes that all light-adapted bR molecules, which contain the all-*trans* isomer of retinal, undergo the identical sequence of irreversible reactions in decaying back to their initial state. The addition of a fifth relaxation, which splits the formation of the blue-shifted peak near 410 nm (the so-called *M* peak) into two relaxations (II and III) with rates which differ by about a factor of 5 (Table 1) is reproducibly required in order to accurately fit the data. We have observed this biphasic decay of the *L* intermediate and the corresponding biphasic rise in absorbance at the *M* peak over a range of solution pH from pH 5 to pH 9 and at temperatures ranging from 5 to 35 C (Hofrichter et al., manuscript in preparation). This relaxation has previously been observed in a number of studies (Lozier and Niederberger, 1977; Nagle et al., 1982; Hanomoto et al., 1984; Mauer et al., 1987 *a*, *b*; Xie et al., 1987; Diller and Stockberger, 1987, 1988). This result argues that more than a single kinetic step is required to form the *M* intermediate from *L*. The most frequent interpretation of this result has been that the cycle is branching to produce two different *M* states (Hanomoto et al., 1984; Diller and Stockberger, 1988) but the possibility that the biphasic decay results from the presence of an additional intermediate in a sequential cycle has not been eliminated.

Fig. 8 *b* shows absolute spectra of the *K*, *L*, and *M* intermediates of the light cycle calculated from the difference spectra shown in Fig. 4 *a*, the absolute spectrum of light-adapted PM in Fig. 8 *a* and our best estimates of the fraction cycling. Because complete photoconversion of bR to *K* is not possible and accurate quantum yield data are lacking for the bR → *K* photoreaction and for the photoreactions of the *K* photoproduct, it is not possible to calculate an accurate value for the fraction of bR which is cycling from the energy density of the excitation source alone. Estimates of the

fraction cycling from the observed spectra can only be based on rather subjective criteria: no species can have a negative extinction coefficient, and one requires reasonable bandshapes for the calculated spectra (Nagle et al., 1982). With this caveat, we have attempted to estimate the fraction cycling from our observed difference spectra. In obtaining this estimate, we are aided by the fact that the measured difference spectra of the *K* photoproduct are extremely reproducible over a wide range of conditions. If we assume that there is no branching back to the parent light-adapted bR molecule before relaxation V, it is then possible to compare the difference spectra of the intermediates obtained at different pH and temperature by normalizing using the *K* − bR difference spectra as an internal reference. The calculated spectra of the *M* intermediate are most dependent on the fraction cycling, since the spectral overlap of the 410 peak produced by the deprotonated Schiff base with the parent light-adapted bR is minimal. We have used the *M* spectra measured at high pH (pH 10.5) and low temperature (10 C) to obtain an absolute spectrum for the *K* intermediate by using the criterion that no spectrum in our entire data set show a negative absorbance at any wavelength. We then make use of the *K* − bR difference spectrum obtained under these conditions and the stability of this difference spectrum to estimate the fraction cycling under other conditions (Hofrichter et al., manuscript in preparation).

The spectrum of the *M* intermediate in Fig. 8 *b* contains, in addition to the peak at 410 nm, a significant absorption peak in the region of the absorption maximum of bR (568 nm). This result suggests that the *M* intermediate coexists with a second species that has a spectrum peaking in the vicinity of 560 nm, characteristic of a protonated Schiff base. Based on the absorption spectra, this peak cannot result from branching back to the parent light-adapted bR molecule during the formation of the *M* intermediate, since this peak cannot be cleanly removed by subtraction of the light-adapted bR spectrum. Our results are, therefore, in agreement with early results with argued for the existence of significant absorption under the parent bR peak in this intermediate state at neutral pH (Lozier et al., 1975; Goldschmidt et al., 1976). They also support a recent time-resolved Raman study which concluded that, at pH 8.0, a roughly equimolar mixture of 13-*cis* protonated and 13-*cis* deprotonated Schiff base retinal was present during the lifetime of the *M* intermediate (Diller and Stockburger, 1987, 1988). In our spectra, the peak near 560 nm in the observed spectrum actually lies slightly to the blue of the bR_{568} peak, leaving open the possibility that it could result from rapid equilibration between a deprotonated *M* intermediate and its *L* precursor, since the *L* peak is blue-shifted relative to the parent bR peak.

The peak of the *K* spectrum in Fig. 8 *b* is shifted from that of the parent bR_{568} by <15 nm, having its peak absorbance at ~582 nm. This sift is significantly smaller than has been estimated from the analysis of other data which have generally placed the peak of the *K* spectrum at ~590 nm (Lozier et al., 1975; Nagle et al., 1982; Mauer et al., 1987 *b*). In these analyses, the fraction cycling was determined from the *M* spectra obtained near neutral pH by minimizing the absorbance under the 570 nm peak, a procedure which necessarily produces values that are smaller than those obtained using the criteria described above. The spectrum of the *L* intermediate peaks at ~560 nm. A more complete discussion of these spectra is forthcoming (Hofrichter et al., manuscript in preparation).

At pH < 8, such as the pH 7.3 conditions used for the present experiments, there is evidence for an additional slow relaxation in our light-adapted samples. In the present data, this slow relaxation can be ascribed to the presence of a small fraction of 13-*cis* retinal in these samples at pH 5–7. Evidence to support this interpretation is obtained from the residual difference spectrum associated with this slow relaxation and from its apparent relaxation rate. The difference spectrum associated with this relaxation (Fig. 4 *a*) is very similar to the light-dark difference spectra (Fig. 7 *c*). The fitted relaxation rate of ~5 s^{-1} (Table 1) is also similar to that obtained when data from dark-adapted samples are fitted with six exponential relaxations. Under these circumstances, the 25 s^{-1} relaxation and the offset remaining at the end of the experiment are fitted with a single relaxation having a rate of ~5 s^{-1}. The amplitude of this component is only ~0.002 o.d. for the light-adapted sample, to be compared with an amplitude of 0.04 o.d. for a fully dark-adapted sample. These results suggest that we are resolving the spectrum of the photoproduct produced by excitation of ~3% of the retinal in the light-adapted sample which is present as the 13-*cis* isomer. Xie at al. (1987) have previously reported the presence of a slow component (50 s^{-1} at 30 C, pH 7) in samples which were rather carefully light adapted, but the spectral changes associated with this relaxation did not resemble light-dark difference spectra.

The observation of an identifiable feature of the 13-*cis* cycle in the data on light-adapted bR raises an important experimental point. Generally, in exploring the photocycle of the all-*trans* isomer, experiments have been carried out under continuous illumination by a monitoring beam which also serves as a light-adapting source. To maintain >99% of the sample in the all-*trans* conformation requires an absorbed flux per retinal chromophore of $100/\phi$ photons in the relaxation time for dark adaptation, where ϕ is the quantum yield for the conversion of 13-*cis* retinal to all-*trans* retinal in light-adapted bR. The present experiments argue that ϕ <0.05, arguing that the required flux is >1 s^{-1}. Under our conditions the duration

of the all-*trans* photocycle is ~10 ms, so the probability of exciting an intermediate in the photocycle under these conditions using this photon flux is ~1%. If we now make the optimistic assumption that the lifetimes of all of the photoproducts of the excited intermediate are ≤10 ms, then there is only a very limited range of power density for the light-adapting source which permits the impurities resulting from both thermal dark-adaptation and the photocycling of kinetic intermediates to be maintained at levels below 1%. Should the light cycle slow down or the rate of the light ⇄ dark relaxation increase, this window closes and it becomes impossible to obtain photostationary conditions in which the levels of such impurities are maintained below 1%. This problem has been addressed in some studies (e.g., Xie et al., 1987) by using an additional preillumination source for light adaptation which can be switched off before photoexcitation.

We now turn to the data on dark-adapted PM and the difference spectra obtained by subtraction of the scaled all-*trans* cycle from the data on dark-adapted PM. First, it is important to note that the scale factor required to remove the light cycle from this data on the dark-adapted mixture is ~0.615, a number that is substantially larger than the fraction of all-*trans* retinal in dark-adapted PM. At the high photon fluxes which we are using (~10 photons absorbed/retinal) there is previous evidence that the observed photocycle of dark-adapted PM is dependent on photolysis energy. The results of Kalisky et al., (1977) can be interpreted as showing that the amplitude of the *M* peak in the photoproduct of dark-adapted PM increases markedly at high photolysis energy. This observation is consistent with our results which require that the fraction of bR cycling in the light cycle is about twice as large as the isomer fraction. The reason for this dependence is not known. One possibility is that the smaller fraction of the 13-*cis* component cycling in the photostationary state results from a higher probability for the reverse photoreaction from the photoproducts of the 13-*cis* component to the parent 13-*cis* molecule. An alternative possibility is that photoexcitation of a photoproduct of the 13-*cis* component by a second photon can initiate a light cycle rather than reisomerization to the dark-adapted state. The results shown in Fig. 5 require that all of the *M* intermediate must cycle through *K*, since the scale factors obtained from the $L - K$ difference spectra are essentially identical to those obtained from the $M - L$ difference spectra. This appears to rule out the possibility of direct formation of an *L* or *M*-like photoproduct from the 13-*cis* component as is suggested by the recent results of Drachev et al. (1988) on reconstituted 13-*cis* bR at high pH. Much more extensive studies as a function of photolysis energy will be required to unambiguously determine the relative amplitudes of the 13-*cis* and all-*trans* photocycles.

The results of Fig. 4 *c* show that the difference spectrum of the initial photoproduct and the products of relaxations I and II are very similar (see footnote 2). Each exhibits a ~600 nm peak in the difference spectrum. This feature remains stable until relaxation III, which occurs at 35 ms. The kinetics of this photocycle are dominated by relaxation III, in which nearly 80% of the amplitude of the difference spectrum disappears. From this result, we can argue (cf. Dencher et al., 1976) that the bulk of the photoproduct recycles to the starting material during this relaxation. The presence of a residual difference spectrum subsequent to this relaxation then requires that the cycle branch at some point before the completion of this relaxation. Relaxations I and II produce only small changes (<.005 o.d.) in the spectra of the PM suspension. Relaxation I produces a small blue shift in the spectrum of the photoproduct. This feature is observed in the subtracted data as a red shift in the $L - K$ difference spectrum for dark-adapted samples (Fig. 5). Relaxation II results in about a 15% decrease in the amplitude of the difference spectrum, with the peak shifting back toward its initial position at 600 nm.

This photocycle is very similar to that reported for bacterio-opsin reconstituted with the 13-*cis* retinal isomer (Dencher et al., 1976; Sperling et al., 1977). Here a long-lived photoproduct, which was named ^{610}C, was observed to decay with a half-time of ~30 ms. The only significant difference in the present results is that the corrected photoproduct difference spectrum (Fig. 7 *c*) is not quite so redshifted and peaks between 603 nm and 605 nm. Based on the striking similarity between these cycles, we can assign the major features of the difference data shown in Fig. 1 *c* to the photoproducts of the 13-*cis* component of the dark-adapted mixture. The preservation of all of the major features of the photocycles of both the all-*trans* and the 13-*cis* components in dark-adapted PM provides strong evidence that there is little, if any, functional interaction between bR molecules in PM which affects their proton-pumping cycle.

Quantitative analysis of the amplitudes of the difference spectra in Fig. 4 *c* shows that between 10 and 15% of the photoproduct of 13-*cis* bR persists to times longer than ~1 s (see footnote 2). The similarity between the difference spectrum of this long-lived component and the light-dark difference spectrum obtained in our light-adaptation experiments (Fig. 7 *c*), argues that this species is, in fact, light-adapted bR. If this assignment is correct then the final relaxation in the photocycle of the 13-*cis* component takes place at the relaxation time of ~2,000 s measured for dark adaptation (Fig. 7 *b*). We can then also make use of the dark → light conversion efficiency obtained from the kinetic data in Fig. 7 *a* to estimate the fraction of the 13-*cis* component of the dark-adapted mixture which is cycling in response to photoexcitation.

The overall conversion efficiency of ~2%, relative to an efficiency per cycled chromophore of 10–15% argues that we are cycling between 13 and 20% of the 13-*cis* bR in our dark-adapted sample.

The spectra of the intermediates in the 13-*cis* photocycle can be calculated from the difference spectrum in Fig. 4 *c*, the absolute spectra for the 13-*cis* component of the dark-adapted mixture and an estimate of the fraction cycling. To calculate the spectrum of the 13-*cis* component we make use of the fraction of 13-*cis* retinal present in the dark-adapted mixture obtained from nuclear magnetic resonance (NMR) Harbison et al., 1984) and chemical analysis (Scherrer et al., 1989). The spectrum calculated using a 13-*cis* fraction of 60% is shown in Fig. 8 *a*. Our best estimates of spectra for the photoproducts of the 13-*cis* cycle are shown in Fig. 8 *c*. The calculated spectra assume that the fraction of 13-*cis* retinal which is cycling is 17%, a value consistent with the conversion efficiency estimated above. The spectra exhibit significant red shifts (~15 nm) and significantly larger peak extinction coefficients when compared with the light-adapted bR spectrum. The calculated spectra are, however, highly dependent on the value used for the fraction cycling, which could possibly be as high as the ~27% used for the light data or as low as 13%. The spectra of the early photoproducts calculated at high cycling fractions (24–27%) are only slightly redshifted from the light-adapted bR spectrum and show comparable peak extinction coefficients. The data do not permit spectra for the "C" intermediate that have significantly redshifted peaks and peak extinction coefficients which are comparable with or smaller than that of light-adapted bR. Spectra exhibiting the latter features have been reported from low temperature studies of the photoproducts of the 13-*cis* component of dark-adapted PM (Balashov and Litvin, 1981).

The small spectral changes observed in relaxations I and II could have a number of possible origins. The most obvious possibility is that these relaxations are a part of the photocycle of the 13-*cis* component of the dark-adapted mixture. Relaxations could result from a change in either protein conformation or protonation state in response to the formation of an all-*trans* chromophore. The early relaxation of the difference spectrum at ~2 μs would not have been observable in the experiments carried out by Dencher et al. (1976) because of inadequate time resolution. An alternative explanation is that there is a structural, spectroscopic or kinetic interaction between the cycling all-*trans* molecules and neighboring molecules in the PM lattice. Substitution of molecules containing 13-*cis* retinal for those containing all-*trans* retinal in the light-adapted membrane could be subtly altering the photocycle of the all-*trans* molecules. It is difficult to argue that a structural interaction produces the red-shift of the immediate photoproduct spectrum. To do so, one must explain why this interaction produces a detectable spectral perturbation only for the *K* photoproduct and that the *L*, and *M* intermediates in which the isomerization state of the chromophore is identical have essentially identical spectra in the two cycles. Spectroscopic interaction between neighboring bR molecules cannot be ruled out, since the increase in the energy denominator in the dipole-dipole interaction between chromophores could result in a decreased interaction between the later intermediates and the ^{610}C photoproduct of the 13-*cis* bR. It is also not possible to rule out the possibility of kinetic interactions, such as changes in the local proton density at the membrane surface, which could slightly change the kinetics of relaxations that involve the uptake or release of protons. Such an interaction could produce relaxation II by subtly altering the kinetics of the $M \rightarrow N \rightarrow O \rightarrow$ bR relaxations of the light cycle at this temperature. To determine whether these small spectral changes are actually a part of the 13-*cis* cycle the studies on reconstituted 13-*cis* bR would have to be repeated with improved accuracy.

The observed photocycle of the 13-*cis* component is consistent with any mechanism which branches before or during the 35 ms relaxation (III) and are thus clearly consistent with the photocycle proposed by Dencher et al. (1976) in which branching occurs in relaxation III. A number of other mechanisms can provide an equally good explanation of the data. The opposite extreme is a heterogeneous one-step photocycle in which branching occurs at the time of photolysis. This model postulates that *cis-trans* isomerization of the chromophore produces at least two distinct molecular species, each of which contains a different isomer of retinal. The major component would necessarily contain the 13-*trans*, 15-*syn* isomer observed by Roepe et al. (1988), but a small fraction of the photoproduct molecules might either actually be light-adapted bR or rapidly relax to the light-adapted state in relaxation I or II. One would then argue that the 13-*trans*, 15-*syn* component exhibits a red-shifted spectrum and decays more rapidly back to the 13-*cis* conformation, than does light-adapted (13-*trans*, 15-*anti*) bR, presumably because its ground state is destabilized either by interactions within the chromophore or by interactions with the host protein matrix. The possibility of the required photoreaction has previously been suggested by Birge and Pierce (1983) as the pathway for formation of the *K* intermediate from light-adapted bR.

There is very little data which argues for or against either of these two extreme models. They might, in principle, be distinguished by multiple pulse experiments. If a light-adapted molecule is rapidly formed by the photolysis pulse, then absorption of a second photon from an intense, shortlived flash could initiate a light cycle of

the all-*trans* photoproduct. If the light-adapted molecule is not formed until the 25 ms relaxation occurs, then photoexcitation of the all-*trans* photoproduct at times <25 ms should not initiate a light cycle, but might convert the photoproduct back to a 13-*cis* species and thereby decrease the total yield of light-adapted molecules. Kalisky et al., 1977 reported experiments in which the photoproduct spectra obtained by excitation of dark-adapted PM with a 10 ns laser pulse were examined on the millisecond time scale over a wide range in photolysis power, which showed that increased power dramatically increases the probability of forming an *M*-like intermediate. This observation is consistent with the existence of a two-photon pathway from the 13-*cis* isomer to the light cycle. On the other hand, double pulse photolysis experiments carried out with a 15 ms delay between pulses were interpreted as showing that exposure of the photolyzed sample to a second pulse decreased the probability of light adaptation (Lozier et al., 1978). This observation appears to support the hypothesis that branching occurs in relaxation III. More complete studies of the effect of additional pulses and/or photolysis energy on the photocycle of dark-adapted PM will be required to clarify the interpretation of these early experiments. A particularly straightforward experiment is to explore the complete kinetics of the photocycle as a function of the photolysis energy. Such experiments would expand on the observations of Kalisky et al. (1977) and may help to clarify the details of the mechanism of light-adaptation.

We thank Prof. D. Oesterhelt for providing the purple membrane used in this study and Drs. Scherrer et al. for a preprint of their manuscript.

Received for publication 14 February 1989 and in final form 12 June 1989.

REFERENCES

Balashov, S. P., and F. F. Litvin. 1981. Photochemical conversions of Bacteriorhodopsin. *Biophysics (Engl. Transl. Biofizika).* 26:566–581.

Birge, R. R. 1981. Photophysics of light transduction in rhodopsin and bacteriorhodopsin. *Annu. Rev. Biophys. Bioeng.* 10:315–354.

Birge, R. R., and B. M. Pierce. 1983. The nature of the primary photochemical events in bacteriorhodopsin and rhodopsin. *In* Photochemistry and Photobiology. A. H. Zewail, editor. Harwood Academic, New York. pp 841–855.

Bogomolni R. A., R. A. Baker, R. H. Lozier, and W. Stoeckenius. 1980. Action spectrum and quantum efficiency for proton pumping in Halobacterium Halobium. *Biochemistry.* 19:2152–2159.

Braiman, M. S., and R. A. Mathies. 1982. Resonance Raman spectra of bacteriorhodopsin's primary photoproduct: evidence for a distorted 13-*cis* retinal chromophore. *Proc. Natl. Acad. Sci. USA.* 79:403–407.

Casadio, R., H. Gutowitz, P. Mowery, M. Taylor, and W. Stoeckenius. 1980. Light-dark adaptation of bacteriorhodopsin in triton-treated purple membrane. *Biochim. Biophys. Acta.* 590:13–23.

Chernavskii, D. S., I. V. Chizhov, R. H. Lozier, T. M. Murina, A. M. Prokhorov, and B. V. Zubov. 1989. Kinetic model of Bacteriorhodopsin photocycle: pathway from M state to bR. *Photochem. Photobiol.* In press.

Dencher, N. A., Ch. N. Rafferty, and W. Sperling. 1976. 13-*cis* and *trans* bacteriorhodopsin: photochemistry and dark equilibrium. Berichte der Kernforschungsanlage Julich GmbH. pp. 1–42.

Diller, R., and M. Stockburger. 1987. A new intermediate in the photocycle of bacteriorhodopsin. *In* Springer Proceedings in Physics, Primary Processes in Photobiology, T. Kobayashi, editor. Springer-Verlag, Berlin. 20:164–172.

Diller, R., and M. Stockburger. 1988. Kinetic resonance Raman studies reveal different conformational states of bacteriorhodopsin. *Biochemistry.* 27:7641–7651.

Drachev, L. A., A. D. Kaulen, V. P. Skulachev, and V. V. Zorina. 1988. Electrogenic photocycle of the 13-*cis* retinal-containing bacteriorhodopsin with an M intermediate involved. *FEBS (Fed. Eur. Biochem. Soc.)* 239:1–4.

Fodor, S. P. A., J. B. Ames, R. Gebhard, E. M. M. van den Berg, W. Stoeckenius, J. Lugtenburg, and R. A. Mathies. 1988. Chromophore structure in bacteriorhodopsin's *N* intermediate: implications for the proton-pumping mechanism. *Biochemistry.* 27:7097–7101.

Hanomoto, J. H., P. Dupuis, and M. A. El-Sayed. 1984. On the protein (tyrosine)-chromophore (photonated Schiff base) coupling in bacteriorhodopsin. *Proc. Natl. Acad. Sci. USA.* 81:7083–7087.

Harbison, G. S., S. O. Smith, J. A. Pardoen, C. Winkel, J. Lugtenburg, J. Herzfeld, R. Mathies, and R. G. Griffin. 1984. Dark-adapted bacteriorhodopsin contains 13-*cis,* 15-syn and all-*trans,* 15-anti retinal Schiffs bases. *Proc. Natl. Acad. Sci. USA.* 81:1706–1709.

Hofrichter, J., J. H. Sommer, E. R. Henry, and W. A. Eaton. 1983. Nanosecond absorption spectroscopy of hemoglobin: elementary processes in kinetic cooperativity. *Proc. Natl. Acad. Sci. USA.* 80:2235–2239.

Hofrichter, J., E. R. Henry, J. H. Sommer, R. L. Deutsch, M. Ikeda-Saito, T. Yonetani, and W. A. Eaton. 1985. Nanosecond optical spectra of iron-cobalt hybrid hemoglobins: geminate recombination, conformational changes and intersubunit communication. *Biochemistry.* 24:2667–2679.

Iwasa, T., F. Tokunaga, and T. Yoshizawa. 1981. Photochemical reaction of 13-*cis* bacteriorhodopsin studied by low temperature spectroscopy. *Photochem. Photobiol.* 33:539–545.

Kalisky, O., C. R. Goldschmidt, and M. Ottolenghi. 1977. On the photocycle and light adaptation of dark-adapted bacteriorhodopsin. *Biophys. J.* 19:185–189.

Lozier, R., R. O. Bogomolni, and W. Stoeckenius. 1975. Bacteriorhodopsin; a light-driven proton pump in Halobacterium Halobium. *Biophys. J.* 15:955–962.

Lozier, R. H., W. Niederberger, M. Ottolenghi, G. Sivorinovsky, and W. Stoeckenius. 1978. On the photocycles of light- and dark-adapted bacteriorhodopsin. *In* Energetics and Structure of Halophilic Microorganisms. S. R. Caplan and M. Ginzburg, editors. Elsevier North-Holland Biomedical Press. Amsterdam. pp 123–141.

Maeda, A. T. Iwasa, and T. Yoshizawa. 1977. Isomeric composition of retinal chromophore in dark-adapted bacteriorhodopsin. *J. Biochem. (Tokyo).* 82:1599–1604.

Mauer, R., J. Vogel, and S. Schneider. 1987*a*. Analysis of flash photolysis data by a global fit with multi-exponentials. I. Determination of the minimal number of intermediates in the photocycle of

bacteriorhodopsin by the 'stability criterion'. *Photochem. Photobiol.* 46:247–253.

Mauer, R., J. Vogel, and S. Schneider. 1987*b*. Analysis of flash photolysis data by a global fit with multi-exponentials. II. Determination of consistent natural rate constants and the absorption spectra of the transient species in the bacteriorhodopsin photocycle from measurements at different temperatures. *Photochem. Photobiol.* 46:255–262.

Murray, L. P., J. Hofrichter, E. R. Henry, M. Ikeda-Saito, K. Kitagishi, T. Yonetani, and W. A. Eaton. 1988. The effect of quaternary structure on the kinetics of conformational changes and nanosecond geminate rebinding of carbon monoxide to hemoglobin. *Proc. Natl. Acad. Sci. USA.* 85:2151–2155.

Nagle, J. F., L. A. Parodi, and R. H. Lozier. 1982. Procedure for testing kinetic models of the photocycle of bacteriorhodopsin. *Biophys. J.* 38:161–174.

Oesterhelt, D., M. Meentzen, and L. Schuhmann. 1973. Reversible dissociation of the purple complex in bacteriorhodopsin and identification of 13-*cis* and all-trans retinal as its chromophores. *Eur. J. Biochem.* 40:453–463.

Press, W. H., B. P. Flannery, S. A. Teukolsky, and W. T. Vetterling. 1986. Numerical Recipies: The Art of Scientific Computing. Cambridge University Press, Cambridge. 818 pp.

Roepe, P. D., P. L. Ahl, J. Herzfeld, J. Lugtenburg, and K. J. Rothschild. 1988. Tyrosine protonation changes in bacteriorhodopsin. *J. Biol. Chem.* 263:5110–5117.

Scherrer, P., W. Stoeckenius, M. K. Mathew, and W. Sperling. 1987. Isomer ratio in dark-adapted bacteriorhodopsin in biophysical studies of retinal proteins. T. G. Ebrey, H. Frauenfelder, B. Honig, and K. Nakanishi, editors. University of Illinois Press, Urbana.

Scherrer, P., M. K. Mathew, W. Sperling, and W. Stoeckenius. 1989. The retinal isomer ratio in dark-adapted purple membrane and bacteriorhodopsin monomers. *Biochemistry.* In press.

Smith, S. O., J. A. Pardoen, P. P. J. Mulder, B. Curry, J. Lugtenburg, and R. A. Mathies. 1983. Chromophore structure in bacteriorhodopsin's o_{640} photointermediate. *Biochemistry.* 22:6141–6148.

Smith, S. O., A. B. Myers, J. A. Pardoen, C. Winkel, P. P. J. Mulder, J. Lugtenburg, and R. A. Mathies. 1984. Determination of the Schiff base configuration in bacteriorhodopsin. *Proc. Natl. Acad. Sci. USA.* 81:2055–2059.

Smith, S. O., I. Hornung, R. van der Steen, J. A. Pardoen, M. S. Braiman, J. Lugtenburg, and R. A. Mathies. 1986. Are C_{14}–C_{15} single bond isomerizations of the retinal chromophore involved in the proton-pumping mechanism of bacteriorhodopsin? *Proc. Natl. Acad. Sci. USA.* 83:967–971.

Sperling, W., P. Carl, Ch. N. Rafferty, and N. A. Dencher. 1977. Photochemistry and dark equilibrium of retinal isomers and bacteriorhodopsin isomers. *Biophys. Struct. Mechanism.* 3:79–94.

Stoeckenius, W. R., and R. A. Bogomolni. 1982. Bacteriorhodopsin and related pigments of halobacteria. *Annu. Rev. Biochem.* 52:587–615.

Stoeckenius, W. R., R. H. Lozier, and R. A. Bogomolni. 1979. Bacteriorhodopsin and the purple membrane of halobacteria. *Biochim. Biophys. Acta.* 505:215–278. Biochim. Biophys. Acta 505:215–278.

Xie, A. H., J. F. Nagle, and R. H. Lozier. 1987. Flash spectroscopy of purple membrane. *Biophys. J.* 51:627–635.